MAX-PLANCK-INSTITUT FÜR PLASMAPHYSIK

GARCHING BEI MÜNCHEN

Single Longitudinal Mode Operation of Pulsed CO_2 Lasers

N.R. Heckenberg

IPP IV/83 July 1975

Die nachstehende Arbeit wurde im Rahmen des Vertrages zwischen dem Max-Planck-Institut für Plasmaphysik und der Europäischen Atomgemeinschaft über die Zusammenarbeit auf dem Gebiete der Plasmaphysik durchgeführt.

IPP IV/83

N.R. Heckenberg

Single Longitudinal Mode Operation of Pulsed CO_2 Lasers

July 1975 (in English)

Abstract

A number of experiments are described which were carried out as part of a program to develop a high power pulsed CO_2 Laser operating on a single transverse and longitudinal mode.

The work described in this report was prompted by the requirements of proposed CO_2 laser small angle scattering experiments using heterodyne detection of the scattered light. For reasons covered in /1/ it would be desirable to use the high power laser source as the source of local oscillator radiation. This however places very severe conditions on the monochromaticity of the pulsed laser output.

Unfortunately the output of high power pulsed CO_2 lasers is usually far from monochromatic. Firstly the laser can operate (even simultaneously) on a number of rotational lines. Then, as a result of pressure broadening the gain width is sufficiently large that within a given line a number of transverse and longitudinal modes can reach threshold as the laser gain rises during and after the discharge pulse. Until saturation is reached these modes can grow independently resulting in laser pulses showing strong intermode beating (fig. 1).

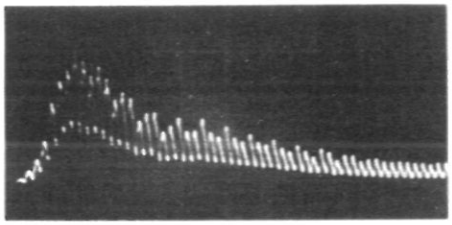

Fig. 1
A typical CO_2-TEA laser pulse (100ns/div) showing beating between longitudinal (56 MHz) and transverse (18 MHz) cavity modes. A Tektronix 454 oscilloscope was used to display the output of a Rofin photon drag detector.

That the high frequency modulation is indeed longitudinal mode beating is demonstrated by its variation with laser length (fig.2).

It is this beating between cavity modes which is of greatest concern here, not only because operation on more than one rotational line can be prevented by incorporating a dispersive element such as a prism or grating in the cavity /2/ but also because the spectrum of light scattered by the plasma would have a width of less than 1 GHz /1/ much less than the separation between rotational lines.

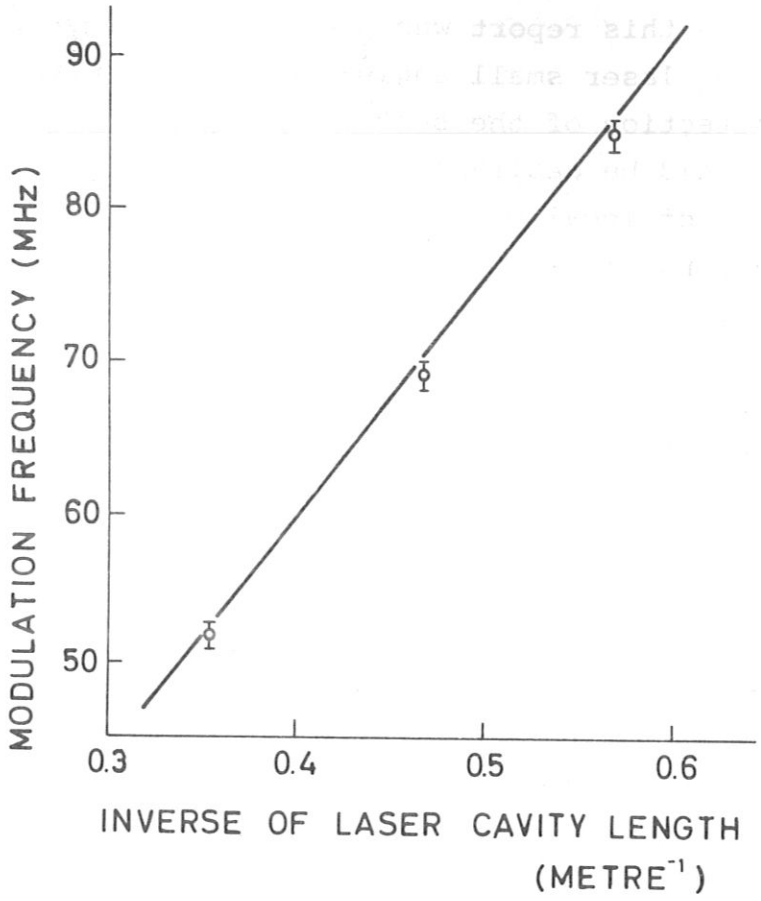

Fig. 2 Variation of CO_2 laser pulse modulation frequency with cavity length. The solid line is the frequency difference $\nu_o = c/2\ell$ between successive longitudinal modes of a cavity of length ℓ .

Cavity Mode Selection

The resonant frequency ν of a cavity mode is given by

$$\nu = \nu_o \left\{ (q+1) + \frac{1}{\pi}(m+n+1)\cos^{-1}\sqrt{\left(1-\frac{\ell}{R_1}\right)\left(1-\frac{\ell}{R_2}\right)} \right\}$$

where the fundamental (longitudinal) beat frequency ν_o is given by $\nu_o = \frac{c}{2\ell}$

Here q is the number of modes of the axial standing wave pattern, m and n are transverse mode numbers (rectangular coordinates) ℓ is the length of the laser cavity and R_1 and R_2 the radii of

curvature of the laser mirrors /4/. The longitudinal modes are usually 50 - 150 MHz apart while the transverse modes are typically separated by about 15 MHz.

It is possible to suppress unwanted transverse modes by introducing an aperture into the cavity. This increases the losses preferentially for higher order modes /3/ leaving the lowest divergence gaussian TEM_{oo} mode little affected, even though the total output power is naturally considerably reduced. This technique works equally well for pulsed and CW lasers.

The suppression of unwanted longitudinal modes is a more difficult problem because the spatial distributions of the different modes are not greatly different /4/.
For discharge pressures above about 10 Torr the gainwidth of the CO_2 laser is determined by pressure broadening at a rate of between 4 and 5 MHz/Torr /5/ so that even with a discharge pressure of 200 Torr the gainwidth is already of the order of a gigahertz. This means that the gain at the longitudinal modes lying adjacent to one at line centre is only 2 % less than the central gain. Thus, following the analysis of Sooy /6/ one expects a ratio of the adjacent to the dominant mode.

$$P_2/P_1 = \left[e^{2(\sigma_2 - \sigma_1) N_o \ell} \right]^p \doteq 3 \times 10^{-2}$$

Should the cavity length drift to where the modes are symmetrically placed about line centre the powers in the two modes will become equal.
Here σ_n is the cross section for stimulated emission at the wavelength of the n th mode, N_o the inversion when threshold is reached, and ℓ the length of laser medium. The number of loop transits p between threshold and saturation is of order 30 /7/ for a CO_2 laser and σN_o is of order 3 %/cm /8/ so that P_2/P_1 is typically more than 0.01. (The resonator length was taken as 2 m, and ℓ = 1 m).
That this performance must be considerably improved is evident from the following simplified argument.

Scattered light (power P_s per unit bandwidth, say) and local oscillator light P_{LO} are incident on a detector. The mixing signal within a certain IF bandwidth B is to be observed.

Firstly assume that the local oscillator is monochromatic but that the laser source consists of two components of powers P_1 and P_2. In this case there will be two scattered light spectra, each centred on its source mode frequency, with intensities proportional to P_1 and P_2. Depending on the accuracy and resolution with which the shape of the spectrum is to be determined a ratio $P_2/P_1 = 0.01$ would probably be quite sufficient to avoid confusion - not too stringent a condition but one already not satisfied by most TEA lasers.

If, however, one hopes to use the high power source laser also as the source of the local oscillator signal the situation is more serious. Then the IF signal in the bandwidth B contains not only the signal generated by the mixing of the local oscillator centre frequency and part of the spectrum of scattered light but also beating between components of the LO itself - the so called homodyne spectrum /9/. For simplicity consider a LO consisting of two laser long. modes with powers P_{LO1} and P_{LO2}. Considering now a bandwidth B centred on the longitudinal mode beating frequency ν_o then to avoid confusion we desire that the signal generated by the mixing of the scattering signal with the dominant mode be greater than that generated by the mixing of the two modes with each other. Then $P_{LO2} < P_s B$

Typically $P_s B \sim 10^{-18}$ W/Hz x 10^7 Hz = 10^{-11} W

and $P_{LO1} \sim$ 1 mW for HgCdTe detectors for example.

Thus we require $\frac{P_{LO2}}{P_{LO1}} \lesssim 10^{-8}$.

This degree of purity is required in a laser of multimegawatt output if scattering from thermal plasma fluctuations is to be observed /1/. The difficulty of achieving such a high output

is compounded by the requirement of a very low divergence beam / 1 / which practically rules out the use of an unstable resonator / 10/.

Longitudinal Mode Selection Experiments

Unfortunately the simple strategy of making the laser sufficiently short that the long. mode spacing $\nu_o = \frac{c}{2\ell}$ is much greater than the gainwidth /11/ is impractical for pulsed CO_2 lasers operating near atmospheric pressure. On the other hand reducing the pressure to about 20 Torr to reduce the linewidth is effective but reduces the power correspondingly. The next most obvious approach is to introduce a frequency dependent loss into the cavity to reduce the cavity loop gain at all but one frequency. A grating does not provide sufficient dispersion to select longitudinal modes although it can be used to select the laser rotational line.
A number of experiments performed to test several mode selection techniques will be described below.

Experimental Laser

Most of the experiments to be described were performed with a small transverse discharge laser of very simple construction which is shown in fig. 3.

A one metre length of 5 cm ID plexiglass tubing acted as discharge vessel and support for two helical rows each of 117 copper pins, between which 2.5 cm long discharges occured. 1000 Ω resistors, one for each pair of pins, helped to distribute the current uniformly.

A mixture of 84 % He, 8 % N_2 and 8 % CO_2 was flowed continuously along the vessel; the pressure was normally held below 300 Torr to obtain diffuse discharges. As the pressure was raised further the interelectrode discharges became more arc-like and no further increase in output was obtained (fig. 4).

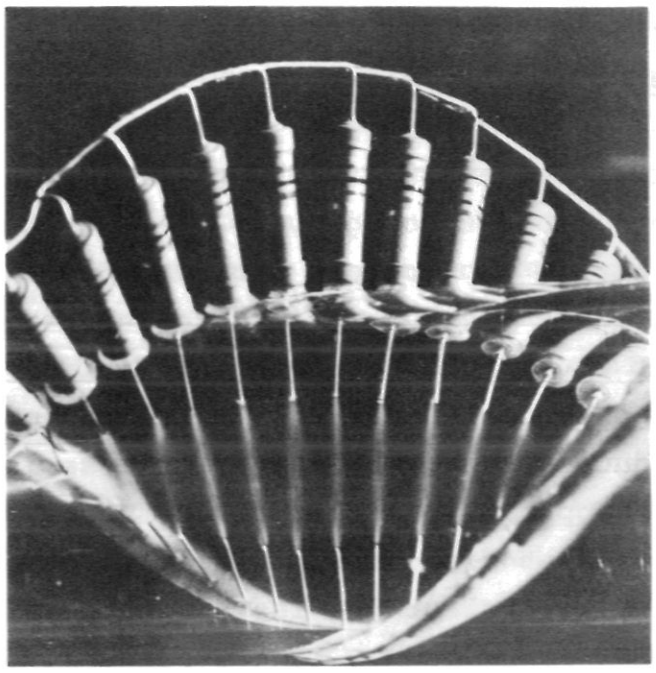

Fig. 3 Laser discharge

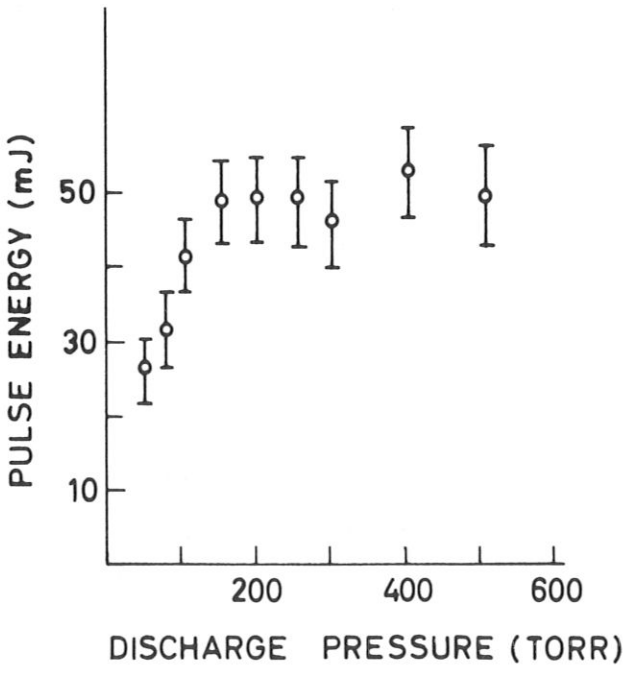

Fig. 4 Laser output energy as function of discharge tube pressure.

The 33 nF capacitor was normally charged to 25 kV.
When discharged a current pulse of 15 A per pin flowed for about 1 μs, the interelectrode voltage drop being about 3 kV. (The carbon block resistors used, although not subject to destruction by the current as carbon film resistors were, suffered internal breakdown which lowered their effective resistance during the current pulse).

The electron collision excitation rates for the upper laser level and the excited nitrogen level /12/ can be determined from the results of Nighan and Bennett /13/ and expressed in terms of energy are 11 kW/cm^3 to the nitrogen and 4 kW/cm^3 to the carbon dioxide.

The laser resonator normally consisted of a gold coated glass or copper curved mirror with a radius of curvature in the range 5 - 10 m and a partially transmitting Ge output flat separated by about 2 m. Usually one mirror sealed one end of the discharge vessel, the other end of which had a Brewster angle NaCl flat.
The laser output pulse power and energy depend on the resonator configuration and output mirror reflectivity, but the energy was typically 100 mJ TEM_{00}.
Some experiments were carried out with a small solid Rogowski profile electrode laser which is described later.

Mode Selection by Intracavity SF_6 Cell

The first experiments using a frequency dependent cavity loss were modelled on those of Nurmikko et al. /14/ where SF_6 which has a strong absorption band near 10 μm with a very fine detailed structure was used as a frequency dependent loss. The experimental setup is shown in fig. 5.

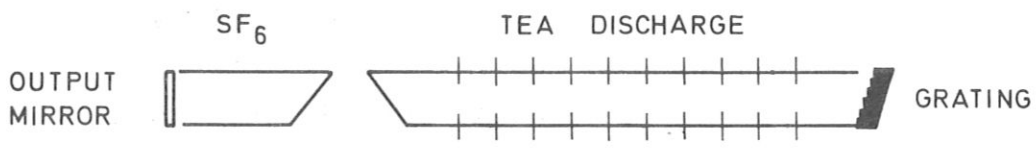

Fig. 5 Single longitudinal mode laser using intracavity SF_6 cell.

Initial experiments carried out with a normal curved mirror in the cavity were unsuccessful because introduction of SF_6 to the absorption cell simply shifted operation from the P(20) to other rotational lines at shorter wavelengths. A curved grating (R=20 m Photo Technical Rsch SF 302 C 1800 grooves/in) was available and thus it was possible to obtain SLM (single longitudinal mode) pulses with 0.05 - 0.1 Torr SF_6 in the 8 cm long absorption cell. It was possible to obtain such pulses on several rotational lines although the laser power was reduced probably mainly because of the smaller cavity mode volume and the imperfect reflectivity of the grating.
A typical pulse is shown in fig. 6.

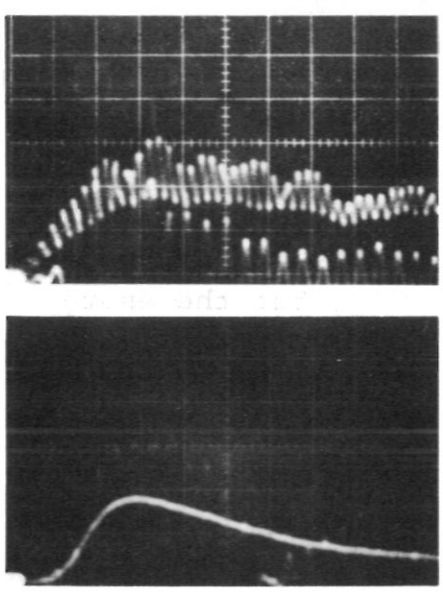

Fig. 6
Output pulses from laser in fig. 5
(50 ns/div)
upper: no SF_6 in cell
lower: 0.1 Torr SF_6 in cell

With the grating, however, fairly reliable elimination of the modulation on the pulses was obtained at the expense of a small reduction in output power on several rotational lines around 10.6 µm. Bleaching of the SF_6 at high powers leads to some accentuation of the sharp gain switched peak at the beginning of the laser pulse.
An intracavity Ge etalon (Lumonics Rsch Model 502) was tried instead of the grating to hold the laser to a rotational line within the absorption band of the SF_6 but was unsatisfactory because operation simply shifted into another one of the etalons passbands near 9,5 µm.

Multimirror Resonators

An elaboration of the simple use of the grating was also tried whereby a partially reflecting Ge mirror was set in front of the grating (fig. 7). This increases the peak reflectivity and should increase the power and selectivity /15/.

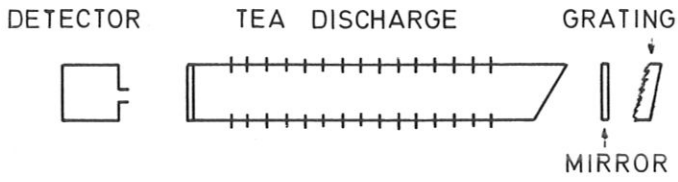

Fig. 7 Single longitudinal mode laser using multimirror resonator

In practice, however, it was difficult to adjust the system to a state where these advantages were realized. Some improvement in mode selection was observed using an 80 % reflective Ge mirror and rather better results using the Ge etalon. The combination of germanium mirror, which is antireflection coated on one side; and grating would constitute a Fabry-Perot resonator whose reflectance shows deep narrow absorption resonances. Thus certain modes might be rejected /16/. The combination of etalon and grating, however, constitutes a three-mirror system, which under certain conditions /17/ can exhibit reflectance enhancements over narrow frequency ranges. A mode lying in one of these ranges will experience smaller losses than the others so that mode selection would be expected to be better within certain critical ranges of adjustment. A pulse, typical of the best performance obtained is shown in fig. 8.

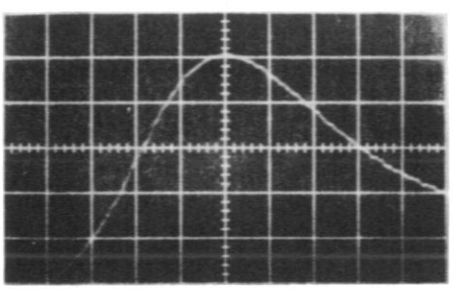

Fig. 8
Output pulse from multimirror laser of fig. 7. (50 ns/div)

It was found impossible to maintain the system alignement well enough to obtain such performance for more than a few minutes at a time.

Hybrid Laser

An alternative to inserting a frequency dependent loss into the cavity is to insert a frequency dependent gain. The minimal obtainable CO_2 laser gainwidth is limited by Doppler broadening to about 60 MHz /18/ but this means that a longitudinal mode on line centre would experience a gain many times that experienced by the adjacent one. (eg. some 30 times more for a 2.7 m cavity) The maximum gain occurring in a pulsed CO_2 laser discharge is usually less than 5 times threshold /19/ so that incorporation of a low pressure (i.e. Doppler broadened) gain tube into the cavity can lead to a quite significant increase in the total gain for just one mode (per rotational line). This is the basic principle behind the hybrid laser /20 - 23/ depicted in fig 9.

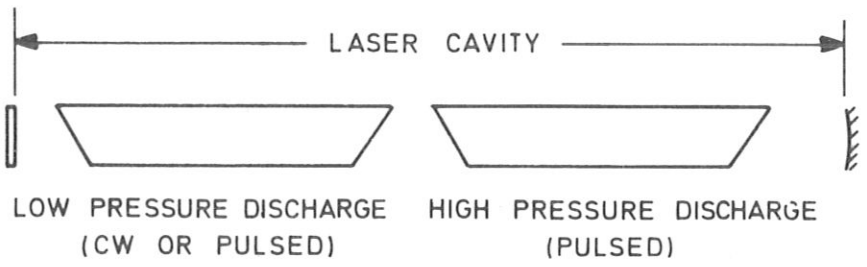

Fig. 9 Schematic diagram of hybrid laser

The low pressure discharge section used is depicted in more detail in fig. 10.

This system, within a wide range of parameters centred on those given in table 1, reliably gave pulses of up to 130 mJ free of longitudinal mode beating as far as could be determined by examination of oscilloscope photographs, even though the output occurred

on different rotational lines depending on the cavity length.

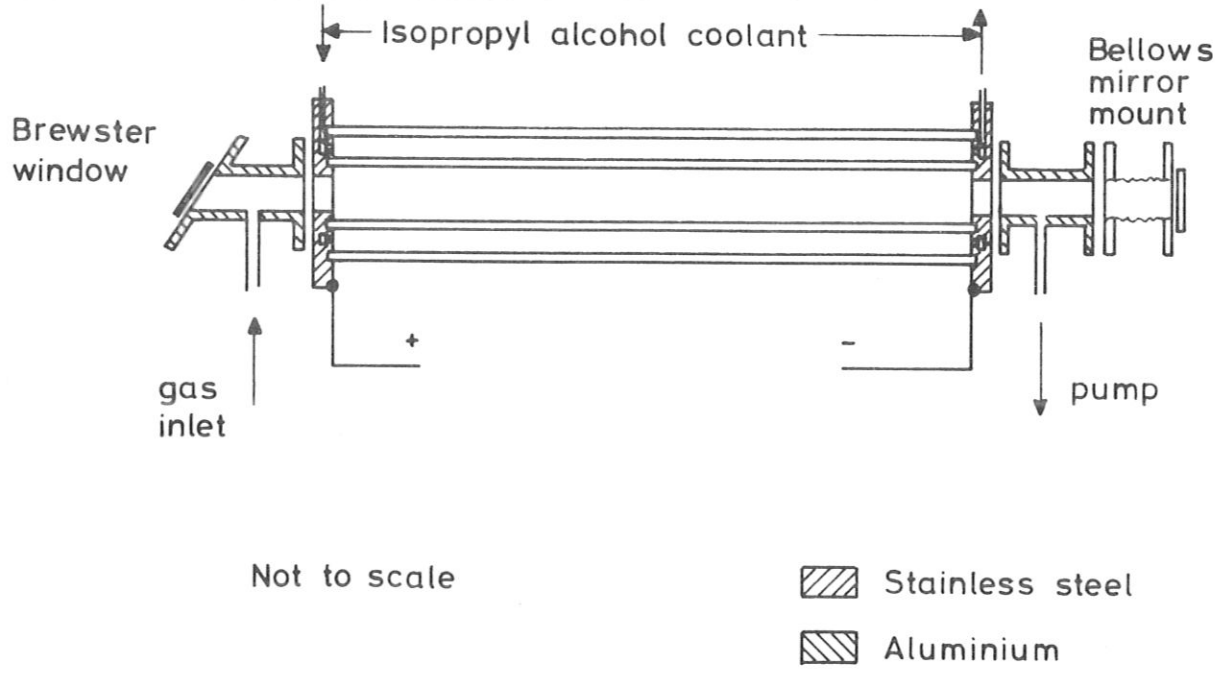

Fig. 10 Low pressure discharge tube used in hybrid laser

Table 1 Operating conditions of hybrid laser using pin-helix discharge

Resonator	Radius of gold coated mirror:	8 m
	Reflectivity of Ge output flat:	80 %
	Length	270 cm
High Pressure Section		
	Pressure	200 Torr
	Gas mix CO_2 : N_2 : He	8 : 8 : 84
Low Pressure Section		
	Pressure	2 Torr
	Gas mix CO_2 : N_2 : He	8 : 8 : 84
	Supply voltage:	4 kV
	Current	15 mA

In view of this reliability, as well as the possibility of altering the pulse shape /22/, further experiments concentrated on the hybrid laser system. Considering the rather different behaviour of the system when the LP section is operated above and below threshold /22/ these two cases are treated separately. Firstly, measurements of the pulse purity made with the LP section below threshold where the poorest performance is expected are described.

Detailed Measurements of Pulse Purity of Hybrid Laser System

The apparatus used for first measurements of the pulse monochromaticity is shown in fig. 11.

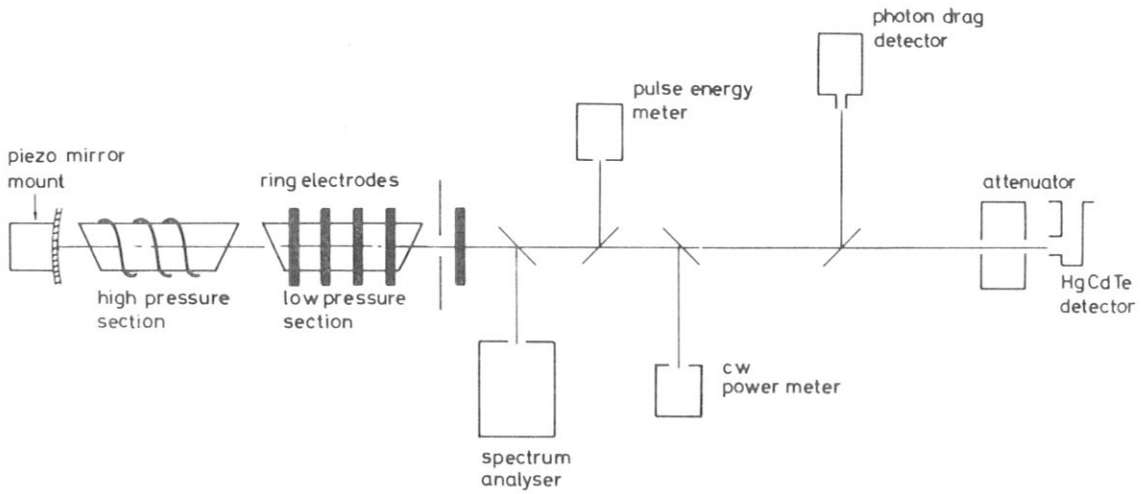

Fig. 11 Apparatus used for measuring residual mode beating in hybrid laser output

Adjustment of the aperture inside the cavity ensured operation in the lowest order transverse mode whilst fine adjustment of the cavity length by means of a piezoelectric mirror mount allowed some degree of rotational line selection so that operation could be confined to the P(20) rotational line.
The low pressure section was fitted with a set of four ring electrodes at different spacings allowing the choice between six different values of gain in the low pressure section.

A system of germanium beamsplitters allowed observation of the laser output by an Opt. Eng. CO_2 laser spectrum analyser, a Rofin photon drag detector, a Gen-Tec pulse energy meter, a Coherent Radiation power meter, and a S.A.T. HgCdTe photovoltaic detector. Care was taken that both fast detectors collected light from the full beam cross section and that the level at the HgCdTe detector, which was biassed, was held below 2 mW to avoid saturation effects. Measurements made during the calibration of the photon drag detector against the HgCdTe detector showed good agreement in the pulse shapes and level of intermode beating. The signal from the photon drag detector was displayed directly on an oscilloscope while that from the HgCdTe detector was fed through a narrow band filter tuned to the frequency corresponding to the cavity longitudinal mode spacing (56 MHz) and a low noise amplifier and was then displayed on a second oscilloscope.

The laser was first observed in the CW mode of operation with the full discharge length and the current was adjusted to bring it just to the threshold of oscillation. Then the discharge length was reduced, keeping the current constant, using the different ring electrodes. In this way it was possible to adjust the gain below threshold in a controlled way, the continuous section gain being proportional to the discharge length. That the discharge is uniform along its length was shown by the fact that the interelectrode voltage drop varied linearly with the length.

Now the high pressure section was pulsed and the laser output observed. Figure 12 shows typical results. The laser pulse energy

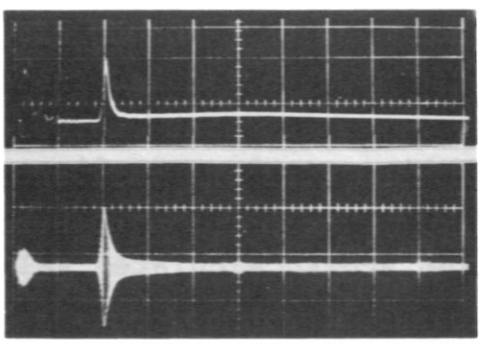

Fig. 12
Typical experimental results in mode beating measurement (2 µs/div)
Upper: photon drag detector signal
Lower: filtered and amplified beat signal from HgCdTe detector

was 75 mJ and the peak power was 10 kW. From the amplitude of the

beat signal observed with the HgCdTe detector and the total pulse power as monitored by the photon drag detector the intensities of the dominant longitudinal mode (I_1) and of the adjacent mode (I_2) and their ratio were determined. (Of course there are two modes spaced 56 MHz from the dominant one, but for our present purposes it is sufficient to speak of one effective mode intensity.) The signal voltage from a square law detector is described by

$$u \propto I_1 + I_2 + 2\,(I_1 I_2)^{1/2} \cos\,(\omega_1 - \omega_2)t$$

Since here $I_1 \gg I_2$ the photon drag detector monitors the first term while the filter ensures that the HgCdTe detector monitors the last term. The experimentally observed intensity ratios are shown in fig. 13 where comparison is made with the theory described below.

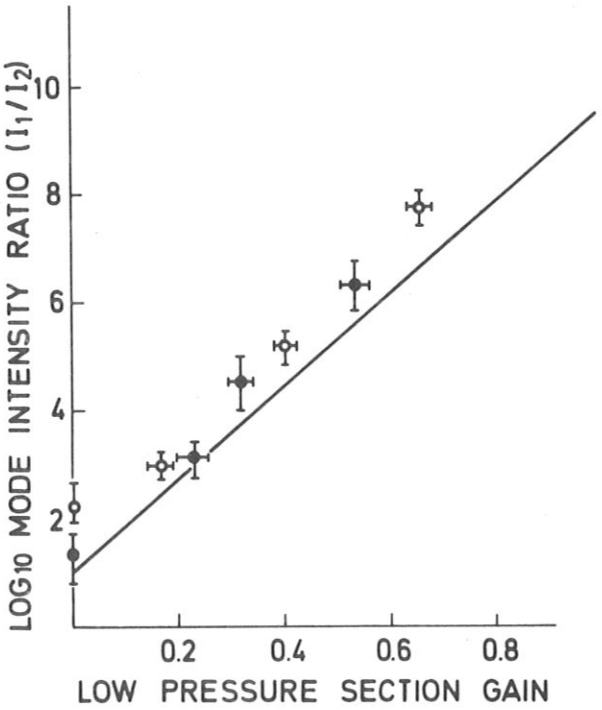

Fig. 13 Ratio of intensities of mode at line centre and adjacent longitudinal mode as function of low pressure section inversion density. The solid line shows calculated values while the points represent measured values. The low pressure section population inversion is expressed as a fraction of the threshold value.

Since the total light intensity at the HgCdTe detector was limited to avoid saturation to about 2 mW, a minimum measurable voltage of 10 μV set a limit on the observable mode rejection ratio at approximately 10^{-9}.

A second run, with the discharge current further reduced, so that the full discharge length no longer corresponded to threshold gain, allowed several more points to be interpolated (open circles in fig. 13.) Since the gain per unit length for these points had been reduced by an unknown factor they were normalized to a straight line fit to the earlier results.
In spite of shot-to-shot variation a clear and rather strong dependence on the low pressure section gain is observed.

Rate Equation Model

Our model is based on that used by Gilbert et al. /19/ for the TEA CO_2 laser, where the kinetics of the processes taking place in the CO_2-N_2-He mixture are analysed in terms of four levels only: upper (a) and lower (b) CO_2 levels, an excited nitrogen level (c), and the ground state. Rate equations are written for the population densities of the three excited states and the cavity photon density, and the set solved numerically. The solutions give an accurate picture of the operation of a conventional TEA laser and the analysis can be easily extended in an approximate way to the hybrid laser /22/.

In the present case we use six equations to describe the molecular level population densities in the two discharges of the hybrid laser, and two to describe the intensities in two cavity modes. We use upper case letters to denote quantities pertaining to the high pressure section and lower case letters for those pertaining to the low pressure section, and consider two cavity modes of intensities I_1 and I_2. Mode 1 is taken to lie at the line centre while for mode 2 the cross sections for emission are decreased by factors F and f in the two sections. For the adjacent longitudinal mode F is approximately unity because of the strong

pressure broadening in the high pressure tube while f is small because of the narrowness of the Doppler broadened gain profile of the low pressure section.

Strictly, since the emission line of the low pressure section is inhomogeneously broadened /24/ three equations are not sufficient to describe its behaviour. However, on the one hand, to attempt to account for the effects of inhomogeneous broadening, would be prohibitively complicated, and on the other, the behaviour of the hybrid laser system, at least when the LP section is operated below threshold, is dominated by what happens in the period between threshold and saturation, during which time the gain of the low pressure section remains constant.

$$\frac{dN_a}{dt} = \sigma c\,(I_1+FI_2)(N_b-N_a) - \Gamma_a N_a + \Gamma_c\,(N_c-N_a) + W_a$$

$$\frac{dN_b}{dt} = \sigma c\,(I_1+FI_2)(N_a-N_b) + \Gamma_a N_a - \Gamma_b N_b + W_b$$

$$\frac{dN_c}{dt} = \Gamma_c\,(N_a-N_c) - \Gamma_{co} N_c + W_c$$

$$\frac{dI_1}{dt} = -\gamma_o I_1 + I_1 \sigma c\,(N_a-N_b) + I_1 \sigma c\,(n_a-n_b) + N_a W_s + n_a w_s$$

$$\frac{dI_2}{dt} = -\gamma_o I_2 + I_2 \sigma cF\,(N_a-N_b) + I_2 \sigma cf(n_a-n_b) + N_a W_s F + n_a w_s f$$

$$\frac{dn_a}{dt} = (I_1+fI_2)\,\sigma c\,(n_b-n_a) - \gamma_a n_a + \gamma_c (n_c-n_a) + w_a$$

$$\frac{dn_b}{dt} = (I_1+fI_2)\,\sigma c\,(n_a-n_b) + \gamma_a n_a - \gamma_b n_b + w_b$$

$$\frac{dn_c}{dt} = \gamma_c\,(n_a-n_c) - \gamma_{co} n_c + w_c$$

σ is the cross section for stimulated emission, c is the velocity of light, and the gammas are collision induced transition rates. $W_{a,b,c}$ and $w_{a,b,c}$ are pumping rates while W_s and w_s are the rates of spotaneous emission into the mode at line centre /19/. γ_o is the inverse of the radiation decay time of the cavity. Using the same rate constants as in /19/ and pumping rates chosen to correspond to those occurring in the experimental laser the equations were solved numerically. For the high pressure section the pumping rates for the upper laser level and the excited nitrogen level were estimated from measurements of the discharge current and voltage as described above. The pumping rate for the lower laser level was set equal to that of the upper /19/. For the low pressure section the required steady pumping rates were chosen by trial and error to give solutions with population inversions lying below threshold when the high pressure section pump terms were set equal to zero. Using such solutions as starting values the equations were solved with the pulsed pumping terms, giving results such as shown in fig. 14 where the intensity in the two modes and the population inversion densities in the two sections are shown. Here F is 0.96 and f is 0.063, corresponding to the experimental situation where the pressure broadened gain width in the high pressure section is 560 MHz (p = 125 Torr) and the Doppler broadened gain width in the low pressure section is 50 MHz (at half height). The cavity length was taken as 2 m. The calculated pulse form is qualitatively correct while the power and pulse energy are within a factor two of those observed.

The variation of the ratio of the intensities of the two modes at the pulse peak as a function of the low pressure section inversion (ie gain) is shown in fig. 13, and is seen to be approximately exponential, a result of the exponential nature of the laser pulse development. As the low pressure section gain approaches threshold, its maximum steady state value, a mode rejection ratio of better than 10^9 is indicated.
The good quantitative agreement of the theoretical results with the experimental observations is probably to some extent fortuitous but indicates at least that the general picture of the operation

of the system is correct and supports the extrapolation of the experimental results to near threshold. It is clear that to achieve optimum performance in a hybrid laser, the low pressure section gain should be as high as possible. Further experiments were performed with a second hybrid laser system using a double discharge high pressure section and will be discussed below.

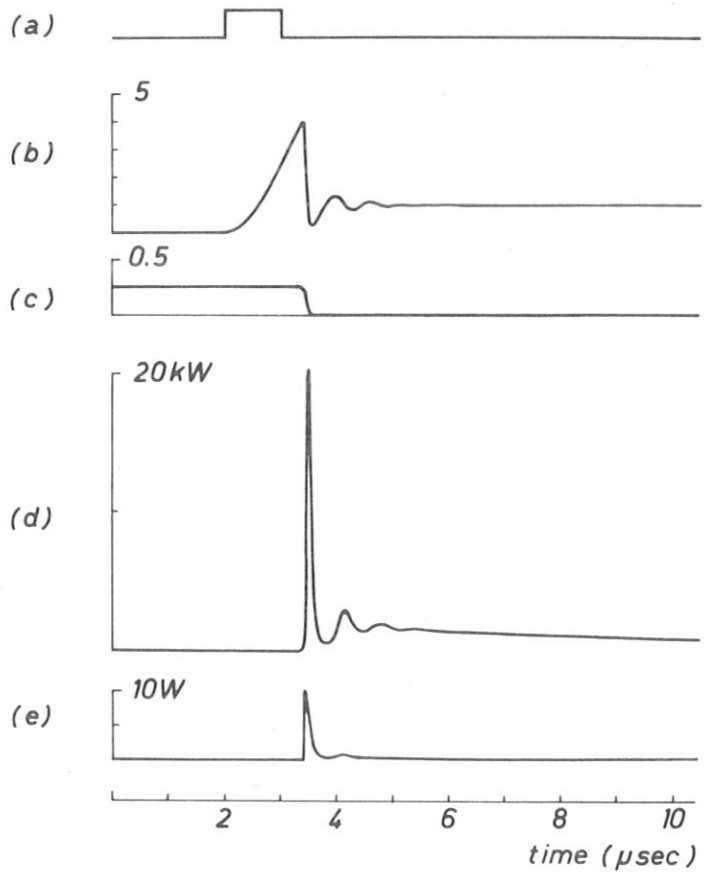

Fig. 14 Numerical solutions of hybrid laser rate equations

(a) pumping of high pressure section

(b) population inversion density ($N_a - N_b$) in high pressure section in units of threshold inversion density

(c) population inversion density ($n_a - n_b$) in low pressure section in units of threshold inversion density

(d) intensity of mode lying at line centre (I_1)

(e) intensity of adjacent longitudinal mode (I_2)

Double discharge high pressure section

The double discharge high pressure section used is depicted in fig. 15.

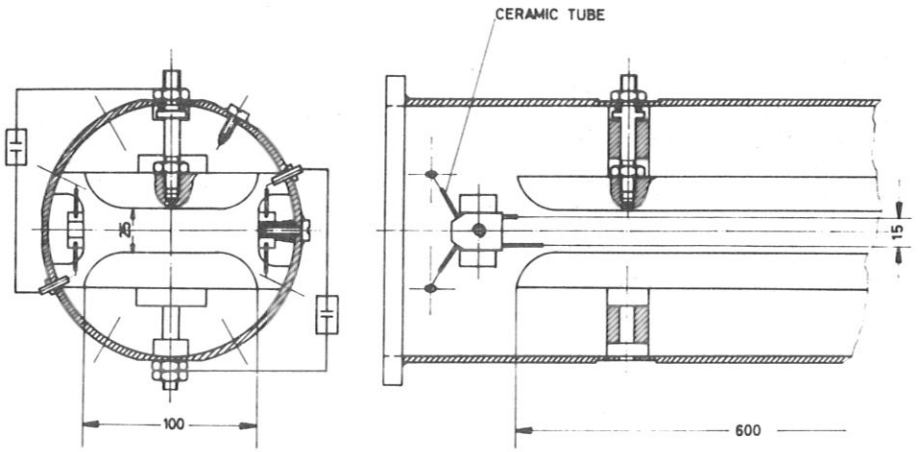

Fig. 15 Double discharge high pressure discharge section

A 25 nF capacitor charged to 50 kV was discharged between two solid aluminium (60 cm x 10 cm) electrodes separated by 2,5 cm /25/. Preionization was provided by four trigger wires connected to the main electrodes through 167 pF capacitors. In initial experiments a second untriggered spark gap in series with the main electrodes served to delay the flow of current between the main electrodes to allow the preionization density to become more uniform. Although some improvement was gained thereby, the addition of a small amount of tripropylamine to the gas mixture /26/ proved so effective in producing uniform arc-free discharges that this complication was unnecessary.

The discharge was normally operated at about 400 T. At higher pressures arcing between the trigger wires reduced the tubes performance. In fact, for the purpose for which the system was originally constructed a long laser pulse was required /27/ so that operation at such low pressures was necessary anyway (see below).

With the low pressure section operated below threshold or switched off a pulse with a high power gain switched peak was observed (fig. 16) with a total energy of up to 100 mJ when a 8 % CO_2, 19 % N_2, and 73 % He gas mixture of 450 T pressure was used. The peak power is approximately 150 kW.

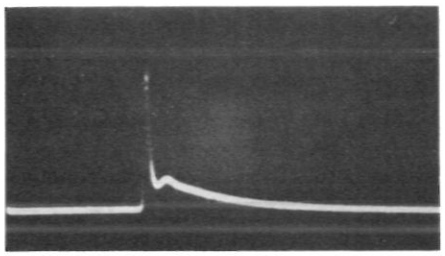

Fig. 16
Output pulse from laser using double discharge high pressure section (2 µs/div). Low pressure section not energized.

Further Pulse Purity Measurements

Measurements of the residual longitudinal mode beating in the pulses of the hybrid laser (below threshold) using the double discharge high pressure section were made following a procedure similar to that described above, with the difference that both pulse shape and mode beating signals were taken from the same HgCdTe detector. This time measurements were made for two different low pressure discharge pressures. When the low pressure section was operated at 1 Torr the laser output pulse appeared on a number of different rotational lines or even mixtures depending on the resonator length. In this case the Doppler broadened gain width of roughly 60 MHz is comparable to the spacing between successive longitudinal modes of the same rotational line, but between these lie modes of other rotational lines. This is demonstrated in fig 17, where the variation in output of the system operated as a CW laser with resonator length is shown. Thus with a low pressure section pressure of 1 Torr the resonator length had to be continually adjusted to maintain operation on the P(20) rotational line. On the other hand, this adjustment has the effect of bringing one cavity longitudinal mode to the centre of the gain profile, under which condition the hybrid laser gives best suppression of unwanted modes. The results obtained are shown in fig. 18.

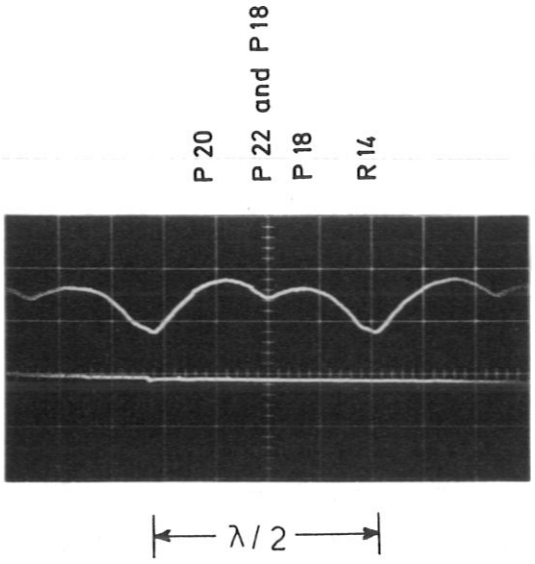

Fig. 17
Variation in output of CW laser as resonator length is varied. An Opt.Eng. CO_2 laser spectrum analyser was used to determine which rotational lines were oscillating.

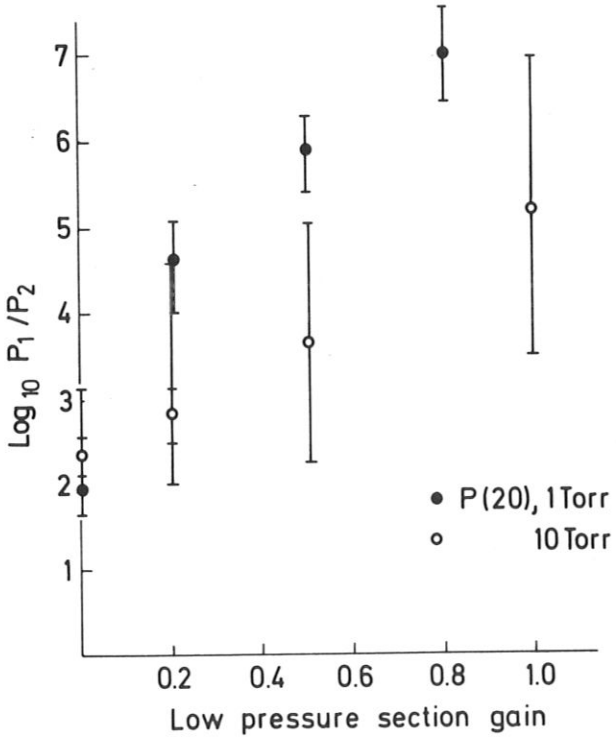

Fig. 18
Variation of hybrid laser output pulse purity with low pressure section gain for two different LP section gain pressures. The logarithm of the ratio of intensities of the main and adjacent modes is plotted against the LP section gain expressed as a fraction of the threshold value.

Not such good performance was observed as with the helix laser, which is probably attributable to the higher gain of the double discharge section. Naturally, the larger the gain in the LP section is compared to the total, the stronger the effect on

unwanted modes will be.

Even poorer performance was observed when the LP section pressure was increased to 10 Torr (fig. 18). Several effects are probably responsible. Firstly the gain width within the LP section is considerably increased by pressure broadening which at this pressure is as important as Doppler. This reduces the difference between the gains experienced in the low pressure section by two modes. Secondly the gain at line centre is reduced although this is counteracted by the effect of the homogeneous pressure broadening allowing the radiation to interact with more of the excited molecules.

Thirdly, and most importantly, the LP section gain width at this pressure is sufficiently larger that the laser pulses always appear on the P(20) line, whether the cavity mode is centred on the LP section gain profile or not. This leads to a very large scatter in the observed amount of residual beating, with the average being considerably worse than that obtained for P(20) pulses obtained with a 1 Torr discharge pressure, but only slightly worse than the average obtained at 1 Torr if the cavity length is allowed to wander arbitrarily (not shown on fig. 18). It seems fair to conclude that operation of the LP section at very low pressures is to be preferred, although, since shortening the laser cavity increases the spacing between longitudinal modes, a much shorter LP section, operated at the higher pressure might perform well if the cavity length could be better stabilized. Of course here the LP section was far longer than it needs to be for operation below threshold. At optimum current with 10 Torr pressure 15 W CW output could be obtained.

Operation above threshold-generation of long pulses

Laser pulses were required to perform an experiment where scattering from 4,5 MHz plasma waves was to be observed /27/. This required, in order to see a significant number of oscillations in the detector IF signal after it had passed through a

350 kHz bandwidth filter, a pulse several microseconds long. Further, since the signal was very small, the Fourier components of the pulse lying within the filter bandwidth had to be minimized. This means that the pulse had to rise and fall as smoothly as possible. A very high degree of longitudinal mode purity was not essentially. The conditions were satisfied using a relatively low pressure (500 T), nitrogen rich (21 %) and carbon dioxide poor (5 %) gas mixture in the HP section and operating the LP section above threshold. Reducing the gain by reducing the proportion of CO_2 in the mix led to a decrease in output energy to about 50 mJ. The pulse power was typically 7,5 kW. Two typical pulses are shown in fig.19.

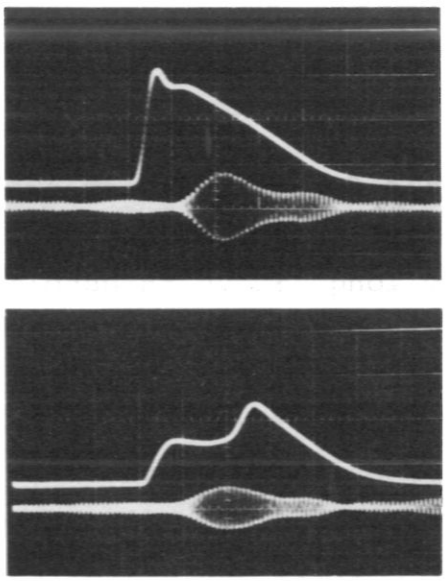

Fig. 19
Typical long pulses from hybrid laser (2 µs/div)
(a) pure P(20)
(b) mainly P(18) with some P(20)

The upper trace in each case is the HgCdTe detector signal showing the pulse shape while the lower is the amplified (60 dB) Fourier component of the pulse lying between within the filter bandwidth. The first pulse (a) is a pure P(20) pulse while the second (b) is a mixture of P(18) and P(20). Such pulses occur when the hybrid laser is operating CW on a rotational line other than P(20), and the high pressure section pressure is sufficiently low that competition between different rotational lines is not strong ie below about 500 T. The gain at P(20) in pulsed lasers seems to be anomalously high /28/ so that normally operation is observed there. In the hybrid laser a standard "above thres-

hold" hybrid laser pulse on a line other than P(20) can have, superimposed on it, a bump, which observation with a monochromator shows to be a P(20) pulse (fig. 20).

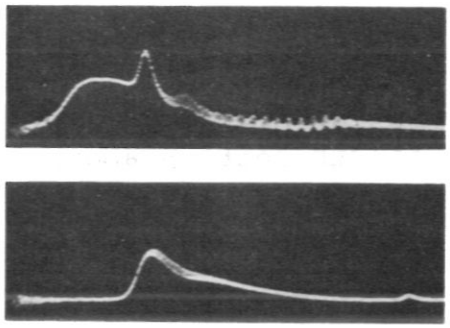

Fig. 20
Hybrid laser pulse (1 µs/div)
Upper: total pulse
(most of energy on P(18))
Lower: pulse observed using CO_2 laser spectrum analyser as a filter to pass only P(20)
(made with pin discharge laser)

Amplification of the Laser Pulse

A Lumonics 601 amplifier module was available for preliminary experiments in amplification of the hybrid laser pulse. Attention was focussed on increasing the power of the long "above threshold" pulse rather than simply achieving maximum peak powers. The output beam of the hybrid laser was passed twice through the amplifier with an input diameter of about 8 mm. After 120 cm of amplification the beam had diverged to a diameter of 15 mm so that the volume of the module was by no means fully utilised. The discharge triggering was arranged so that all or only part of the hybrid laser pulse could be amplified. Because the amplifier can only be operated at atmospheric pressure, the energy stored in the upper laser level and the excited nitrogen molecules are dissipated by collisions within a few tens of microseconds so that amplification occurs only within this time. Some typical pulses are shown in fig. 21. The amplifier used a 7 % CO_2, 15 % N_2, and 78 % He gas mixture. The input pulse had an energy of 35 mJ and maximum power of 7 kW. The output pulse had an energy of up to 350 mJ and a peak power of 70 kW. Since saturation of CO_2 amplifiers seems to normally occur at about 0.4 J/cm^2 /29/ the beam would have to be expanded to amplify higher power oscillator pulses.

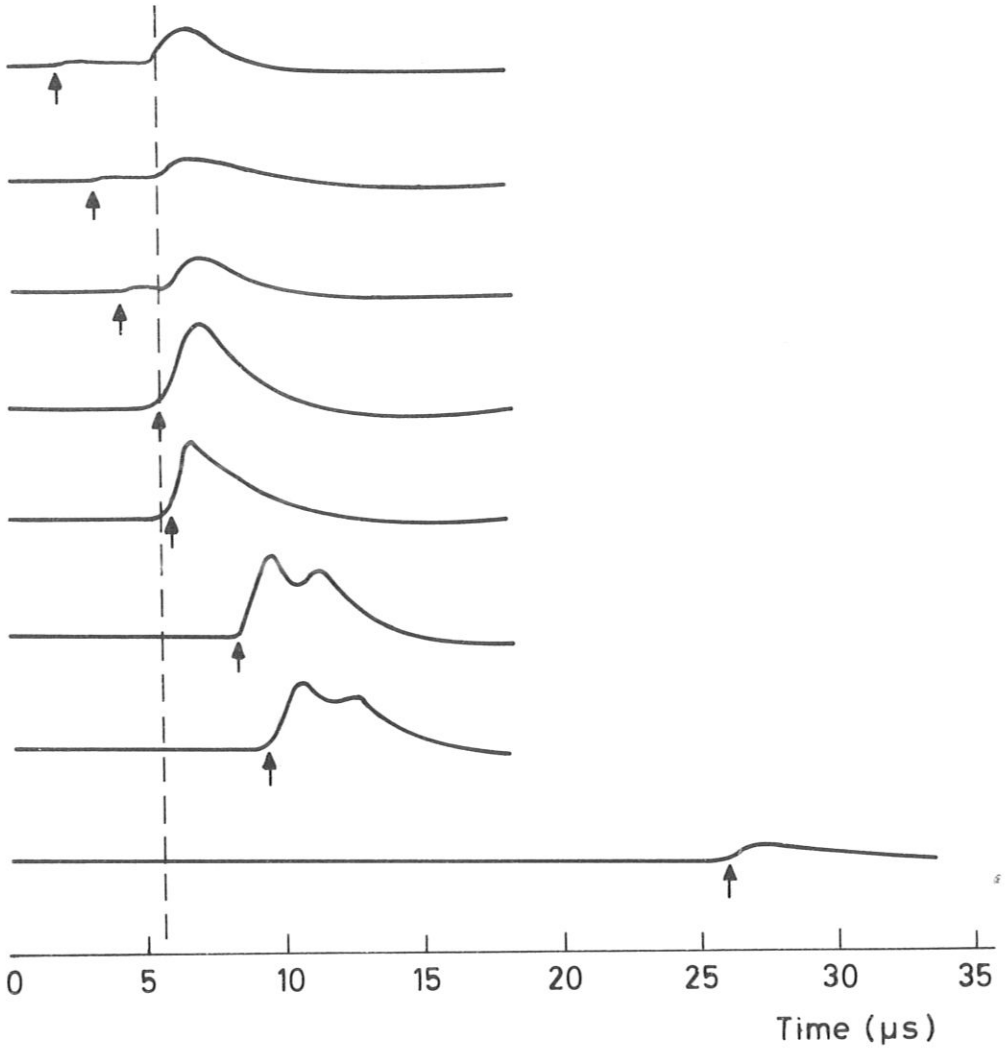

Fig. 21 Amplification of hybrid laser pulses: the beginning of the oscillator pulse is marked by a small arrow. In each case the Lumonics amplifier is fired at t = 5,6 μsec.

Further Improvements to be made

In order to obtain high power monochromatic pulses for experiments where scattering from fluctuations in the 100 MHz range is to be observed a system basically as shown in fig. 22 is proposed.

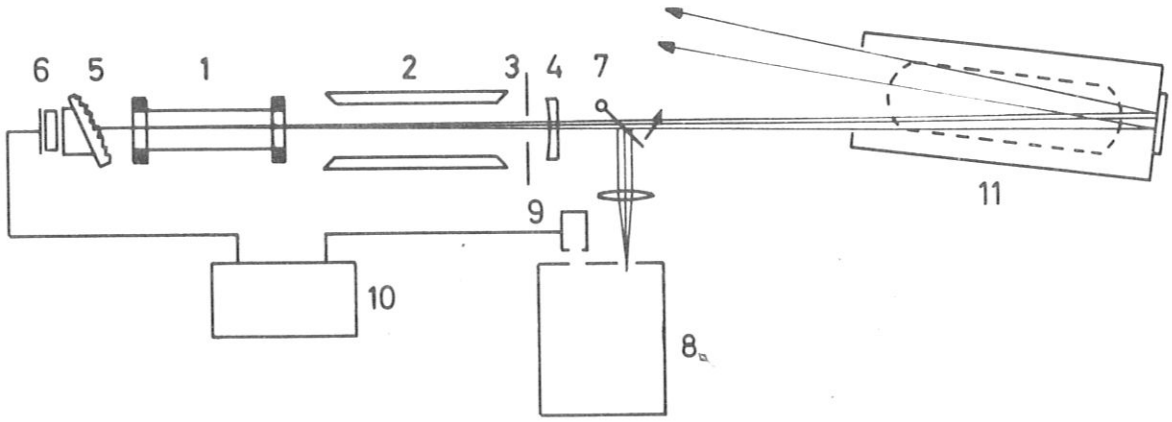

Fig. 22 Possible Laser for Scattering Experiments

1. Low pressure section
2. High pressure section
3. Transverse mode selection aperture
4. Curved Ge output mirror
5. Grating
6. Piezoelectric mount
7. Flip-up mirror synchronized to reduction of current in (1)
8. Monochromator
9. Detector eg pyroelectric
10. Stabilizer unit
11. Amplifier

The experiments described above show that there is a trade-off in the hybrid laser between mode purity and high pressure section gain and output power. Therefore an oscillator-amplifier system is envisaged with an oscillator output of order 50 kW. The high pressure section would be run with a mixture weak in CO_2 and N_2 to keep its gain low and to reduce the nitrogen aftertail although this reduction would not be absolutely necessary. Such an output could be obtained from a laser of the size presently used - indeed such powers have been commonly exceeded. The low pressure section would be operated at about 1 Torr and would be somewhat shortened from its present one meter length, allowing the cavity to be shortened, which should improve the performance somewhat.

The greatest problem would be to stabilize the laser length to ensure that one cavity mode lies at the centre of the low pressure section gain profile. Perhaps the simplest way to do this would be to run the LP section discharge above threshold, stabilizing the cavity length using standard techniques to the centre of a P(20) mode, then reducing the gain of the LP section below threshold some milliseconds before firing the HP section. The stabilization would be simplified if a grating were used to restrict operation to the P(20) rotational line. An alternative might be to stabilise the CW laser output to the centre of the absorption line of a passive CO_2 cell.

A curved output mirror would be used to obtain a large diameter expanding output beam which would be amplified by the Lumonics module about thirty times to a peak power of 1,5 MW. It may even be possible to use the one Lumonics module as not only the amplifier but also the high pressure section of the oscillator. The convenience of this arrangement has to be weighed against the flexibility of two separately triggered discharges.

References

/ 1/ A. Gondhalekar and F. Keilmann, Report IPP IV/26 Institut für Plasmaphysik, Garching (1971), Optics Communications, 14, 4, 263. (1975)

/ 2/ C. Bordé and L. Henry IEEE J. Quantum Electronics, QE-4, 11, 874 (1968)
G. Moeller and J. Dane Rigden, Appl. Phys. Lett. 8, 69 (1966)

/ 3/ P.W. Smith, Proc. IEEE, 60, 4, 422 (1972)

/ 4/ H. Kogelnik and T. Li, Appl. Optics, 5, 10, 1550 (1966)

/ 5/ E.T. Gerry and D.A. Leonard, Appl. Phys. Letters, 8, 227 (1966)

/ 6/ W.R. Sooy, Appl. Phys. Letters, 7, 2, 36 (1965)

/ 7/ J.A. Beaulieu, Proc. IEEE, 59, 4, 667 (1971)

/ 8/ J-L. Lachambre, J. Gilbert, F. Rheault, R. Fortin, and M. Blanchard, IEEE J. Quantum Electronics, QE-9, 4, 459(1973)
N.H. Burnett and A.A. Offenberger, J. Appl. Phys., 44, 8, 3617 (1973)
D.L. Franzen and D.A. Jennings, J. Appl. Phys. 43, 2, 729 (1972)

/ 9/ H.Z. Cummins and H.L. Swinney, Progress in Optics, VIII, 133 (1970)

/10/ A.E. Siegman, Proc IEEE, 53, 277-287 (1965)
W.F. Krupke and W.R. Sooy, IEEE J. Quantum Electronics, QE-5,12, 575 (1969)

/11/ G.E. Stillman, M.D. Stirkis, J.A. Rossi, M.R. Johnson, and N. Holonyak, Appl. Phys. Lett., 9, 268, (1966)

/12/ P.K. Cheo, in "Lasers", A.K. Levine and A.J. DeMaria, ed., Vol. 3, 111, Dekker, N.Y.,(1971)

/13/ W.L. Nighan and J.H. Bennett, Appl. Phys. Lett., 14, 8, 240 (1969)
W.L. Nighan, Phys. Rev. A, 2, 5, 1989, (1970)
S.J. Kast and C. Cason, J. Appl. Phys., 4, 1631, (1973)

/14/ A. Nurmikko, T.A. DeTemple, and S.E. Schwarz, Appl. Phys. Letters, 18, 4, 130, (1971)
T. DeTemple and A. Nurmikko, Optics Communications, 4, 3, 231, (1971)

/15/ J.E. Bjorkholm, T.C. Damen, and J. Shah, Optics Communications, 4, 4, 283, (1971)

/16/ J.A. Weiss and L.S. Goldberg, IEEE J. Quantum Electronics, QE-8, 757 (1972)

/17/ W. Wiesemann, Appl. Optics, 12, 12, 2909, (1973)

/18/ T.J. Bridges, H.A. Haus, and P.W. Hoff, IEEE J. Quantum Electronics, QE-4, 777 (1968)

/19/ J. Gilbert, J.L. Lachambre, F. Rheault, and R. Fortin, Can. J. Phys., 50, 2523, (1972)

/20/ T. DeTemple and A. Nurmikko, Optics Communications, 4, 3, 231, (1971)

/21/ A Gondhalekar, E. Holzhauer, and N.R. Heckenberg, Phys. Letters, 46 A, 3, 229 (1973)

/22/ A Gondhalekar, N.R. Heckenberg, and E. Holzhauer, IEEE J. Quantum Electronics, QE-11, 3, 103 (1975)

/23/ A. Girard, Optics Communications, 11, 4, 346 (1974)

/24/ W.R. Bennett, Jr. Phys. Rev., 126, 580, (1962)

/25/ H.J. Seguin, K. Manes, and J. Tulip, Rev. Sci. Inst., 43, 8, 1134, (1972)

/26/ H. Baumhacker, H. Brinkschulte, E. Fill, C. Grigoriu, W. Schmid, IPP Report 4/123, Institut für Plasmaphysik, Garching (1975)

/27/ D.R. Baker, N.R. Heckenberg, and J. Meyer, Phys. Letters, 51A, 3, 185, (1975)

/28/ H. Brinkschulte and R. Lang, Phys. Letters 47A, 455,(1974)

/29/ J-L. Lachambre, J. Gilbert, F. Rheault, R. Fortin, and M. Blanchard, IEEE J. Quantum Electronics, QE-9,4,459(1973)
D.L. Franzen and D.A. Jennings, J. Appl. Phys., 43, 2,729,(1972)
A. Girard and H. Pépin, Optics Communications, 8, 1, 68,(1973)

Acknowledgements

Various parts of the work described were carried out in collaboration with Dr. D.R. Baker, Dr. J. Meyer, Dr. A Peratt, and Dr. R. Watterson. The expert technical assistance of Mssrs. W. Breitel and J. Prechtl made the experiments possible.